Experimental Investigation into Factors Influencing Methane Hydrate Formation and a Novel Method for Hydrate Formation in Porous Media

ARTICLE *in* ENERGY & FUELS · JULY 2013

Impact Factor: 2.79 · DOI: 10.1021/ef400720h

8 AUTHORS, INCLUDING:

Xiao-Sen Li
Chinese Academy of Sciences
94 PUBLICATIONS **1,423** CITATIONS
SEE PROFILE

Wenyue Xu
Schlumberger Limited
42 PUBLICATIONS **808** CITATIONS
SEE PROFILE

Gang (Kevin) Li
Monash University (Australia)
275 PUBLICATIONS **3,540** CITATIONS
SEE PROFILE

Jing-Chun Feng
Chinese Academy of Sciences
13 PUBLICATIONS **50** CITATIONS
SEE PROFILE

energy&fuels

Article

pubs.acs.org/EF

Experimental Investigation into Factors Influencing Methane Hydrate Formation and a Novel Method for Hydrate Formation in Porous Media

Yi Wang,[†,‡,§] Xiao-Sen Li,[*,†,‡] Wen-Yue Xu,[∥] Qing-Ping Li,[⊥] Yu Zhang,[†,‡] Gang Li,[†,‡] Ning-Sheng Huang,[†,‡] and Jing-Chun Feng[†,‡,§]

[†]Key Laboratory of Renewable Energy, Guangzhou Institute of Energy Conversion, and [‡]Guangzhou Center for Gas Hydrate Research, Chinese Academy of Sciences, Guangzhou 510640, People's Republic of China

[§]University of Chinese Academy of Sciences, Beijing 100083, People's Republic of China

[∥]Schlumberger Limited, Sugar Land, Texas 77478, United States

[⊥]CNOOC Research Center, Beijing 102227, People's Republic of China

ABSTRACT: The behaviors of methane hydrate formation in porous media are investigated in three-dimensional vessels. The effects of the fugacity difference, the water−gas ratio, and the volume of the vessel on the formation rate of methane hydrate are studied. The results show that the formation rates are disproportionate to the fugacity differences but in proportion to the volume of the vessel and the change of the initial gas−water ratio has little effect on the rate of hydrate formation. Meanwhile, according to the discussion about the temperatures and resistances in hydrate reservoir, it is confirmed that methane hydrate forms from the boundaries to the center of the vessel. Furthermore, a new method is designed to form methane hydrate samples in porous sediments with high hydrate/water saturation and low gas saturation.

1. INTRODUCTION

Methane hydrates are a kind of non-stoichiometric, crystalline compound formed by water and methane molecules with high pressures and low temperatures.[1,2] The methane hydrate reservoirs have been found all over the earth, which are vastly distributed in the permafrost and offshore areas.[3−5] The reserve of natural gas in hydrate deposits is estimated to be twice that of all fossil fuel reserves available worldwide and is considered as a potential asset.[6] The methods for recovering natural gas from hydrates are various and still developing. The most practical methods are the thermal stimulation method,[7−9] the depressurization method,[10−12] and the chemical inhibitor injection method.[13] In addition, the CO_2 replacement,[14] in which the liquid CO_2 is injected into hydrate reservoirs to replace the methane gas, has been developed recently.

The research communities mainly focus on prospecting for hydrate resources and improving technology to produce gas from gas hydrate deposits. However, only a few studies present the laboratory data about the methane hydrate formation. In fact, hydrate formation behaviors in porous media are also important for the studies about drilling and seismic observations of natural gas hydrates.[15] Meanwhile, gas hydrate formation is considered as a nuisance in deepwater−oil/gas production from a safety perspective. For example, in 2010, gas hydrate formation was the cause for the failure of a 100 ton containment structure following the Macondo well blowout in the Gulf of Mexico.[16]

Christiansen and Sloan[17] investigated the kinetics and process of hydrate formation. Kvamme[18] reported nucleation theory for the kinetics of hydrate formation and growth based on the multicomponent diffusive interface theory. Kneafsey et al.[19] performed a series of experiments to study hydrate formation in a large X-ray transparent pressure vessel. Linga et al.[20] established an apparatus with a variable volume bed of silica sand particles to study the hydrate formation. Independent verification of hydrate formation is observed by Raman spectroscopy in experiments. Zhou et al.[21] presented hydrate formation data in the water-saturated silica sand matrix conducted at 2.2 °C and 4137 kPa in a 72 L vessel. Yang et al.[22] designed a method to form hydrate homogeneously distributed in sediment. In this method, they used frozen sand instead of wet sand with pore water. However, few studies about the research on the rate of methane hydrate formation in porous media have been reported. Meanwhile, most of the naturally occurring gas hydrates that have been proven are with a low saturation of gas,[23] whereas the hydrate simples are always with a high saturation of gas in the current experimental simulation on the hydrate dissociation, because the hydrate simples with low gas saturation are hard to obtain.

In this work, the methane hydrate formation in porous media was investigated and the three-dimensional data on the hydrate formation behaviors were presented. In the experiments, the effects of the pressure, the gas−water ratio, and the volume of the vessel on the formation rate of methane hydrate were studied. Finally, we designed a method to form methane hydrate samples in porous sediments with high hydrate/water saturation and low gas saturation.

Received: April 21, 2013
Revised: June 8, 2013
Published: June 12, 2013

   dx.doi.org/10.1021/ef400720h | *Energy Fuels* 2013, 27, 3751−3757

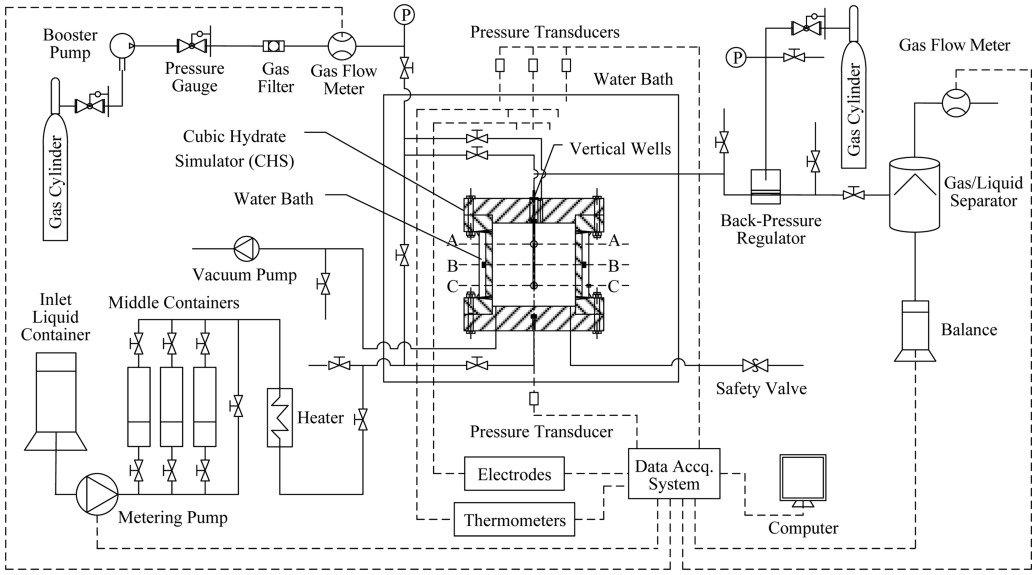

Figure 1. Experimental apparatus.

2. EXPERIMENTAL SECTION

2.1. Experimental Apparatus. The schematic of the apparatus is shown in Figure 1, which has been used to investigate methane hydrate production by the huff and puff method[24] and the depressurization method.[10] The experimental apparatus involves a high-pressure reactor, a water bath around the reactor, a back-pressure regulator, a gas and liquid injection equipment, a water/gas separator, a data acquisition system, and some measurement units. The core component of the apparatus is the high-pressure reactor. In this work, two reactors with different sizes, which are the pilot-scale hydrate simulator (PHS) and cubic hydrate simulator (CHS), are used for investigating the hydrate formation. The details of the experimental apparatuses have been reported in our previous work.[10,12,25−28]

2.1.1. Pilot-Scale Hydrate Simulator (PHS). The PHS is a cylindrical pressure vessel (0.60 m in length and 0.50 m in diameter) with the inner volume of 117.8 L. Figure 2a gives the schematic plot of the inner PHS and the well design in the PHS. There are 7 × 7 × 3 = 147 thermocouples on three horizontal layers (layer A−A, layer B−B, and layer C−C) in the PHS. The name of each thermocouple could be illustrated as follows: The 49th thermocouples on layer A−A to layer C−C are named T49A, T49B, and T49C, respectively. The accuracy of the thermocouple is ±0.1 °C in this work.

2.1.2. Cubic Hydrate Simulator (CHS). The CHS is cubic inside (inner volume of 5.8 L and maximum pressure of 25 MPa). The distributions of the thermocouples (measure temperatures), electrodes (measure resistances), and production wellheads within the CHS are shown in Figure 2b. As seen in Figure 2b, there are 25 × 3 thermocouples, 12 × 3 electrodes, and one central vertical well in the CHS. There are three layers, which divide the measuring points and the wellheads, named layer A, layer B, and layer C, respectively.

2.2. Experimental Procedure. *2.2.1. Hydrate Formation.* In this work, the porous sediments are the silica sands with the particle size from 300 to 450 μm. Before the experiments start, the silica sand is placed in the vessels as the porous media and porosities are approximately 48%. The vessels are emptied twice to remove the residual air. Then, volumes of deionized water are injected into the systems by the metering pump. Meanwhile, the temperature of the water bath is set to a predetermined temperature required for the gas hydrate synthesis, which is 8.5 °C in this work. Methane gas is then injected to pressurize the vessels to 20 MPa. Afterward, the inlet and outlet valves of the vessels are closed to keep the system in a constant volume condition. When hydrate formation starts, the pressures inside the reactors decrease. The hydrate formation processes last for 10−20 days. During the hydrate formation, the temperatures, the pressures, and the electric resistances in the vessel are recorded at 5 min intervals by the data acquisition system.

According to the reaction equation of hydrate formation, the moles of hydrate formation (N_{ht}) are equal to the moles of methane consumed (N_{gt}) at time t, which can be expressed as

$$N_{ht} = N_{gt} \tag{1}$$

The moles of methane consumed in the reactors can be calculated using the pressure and temperature data,[20] which is shown as follows:

$$N_{gt} = \left(\frac{PV}{zRT}\right)_{gi} - \left(\frac{PV}{zRT}\right)_{gt} \tag{2}$$

where z is the compressibility factor, $(PV/zRT)_{gi}$ is the initial moles of the methane in the reactors, and $(PV/zRT)_{gt}$ is the remaining moles of the methane in the reactors at time t.

Subsequently, the rate of hydrate formation is given by

$$R_{ht} = \left(\frac{dN_h}{dt}\right)_t = \frac{N_{h,t+\Delta t} - N_{ht}}{\Delta t}, \quad \Delta t = 5 \text{ min} \tag{3}$$

Furthermore, hydrate saturation (S_h) is calculated as the volume ratio of hydrate and available pore space and expressed as follows:

$$S_h = \frac{N_h M_h}{\rho_h V_\phi} \tag{4}$$

where M_h is the molecular weight of the hydrate, which is 124 g/mol, ρ_h is the density of hydrate, which is 0.94 g/cm^3, and V_ϕ is the available pore space, which is 2752 mL in this work.

2.2.2. Hydrate Formation with High Hydrate/Water Saturation and Low Gas Saturation. A novel method is developed to obtain hydrate samples with high hydrate/water saturation and low gas saturation expediently in this work. The details of this method are described as follows: (1) The amounts of methane (N_g^0) and water (N_w^0), which are used to form hydrate, are calculated from the designed final gas/water/hydrate saturations ($s_g/s_w/s_h$)

$$N_g^0 = V_\phi s_g / v_g + V_\phi s_h \rho_h / M_h,$$
$$N_w^0 = V_\phi s_w \rho_w / M_w + n V_\phi s_h \rho_h / M_h \tag{5}$$

where v_g is the molar volume (m^3/mol) for methane under the local condition, ρ_g is the density of water, which is 1 g/cm^3, M_w is the molecular weight of the water, which is 18 g/mol, and n is the coefficient of the hydrate formation reaction, which is 6.0 in this work. (2) The methane of N_g^0 is injected into the vessel, and a certain

dx.doi.org/10.1021/ef400720h | Energy Fuels 2013, 27, 3751−3757

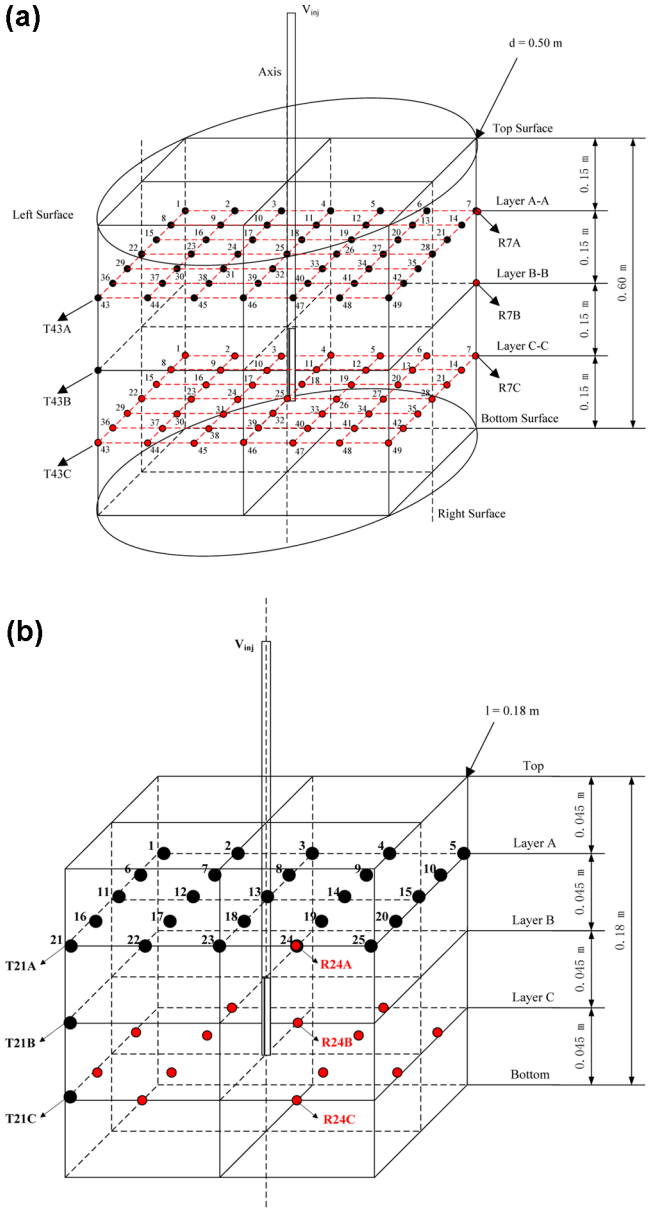

Figure 2. Schematic of distributions of the thermocouples, electrodes, and well in the (a) PHS and (b) CHS.

amount of water is injected into the vessel to pressurize the system to 20 MPa. (3) The inlet is closed to keep the vessel in a constant volume condition for hydrate formation until the system pressure decreases to 15 MPa. (4) The processes of water injection and hydrate formation are repeated until all of the water is injected into the vessel. (5) When the system pressure decreases to the designed pressure, the hydrate sample with designed hydrate/water/gas saturation is formed. The experiment is carried out in the PHS. During this experiment, the temperatures and pressures in the vessel are recorded in the data acquisition system every 30 min.

3. RESULTS AND DISCUSSION

3.1. Reference Case of Hydrate Formation. The reference experiment is carried out in the CHS. Before the methane hydrate forms, 15.8 mol of methane and 1050 g of water are injected into the CHS. Figure 3 shows the change of the system pressure and the cumulative amounts of hydrate formation in the reference case. As seen in Figure 3, methane hydrate rapidly forms and the system pressure gradually

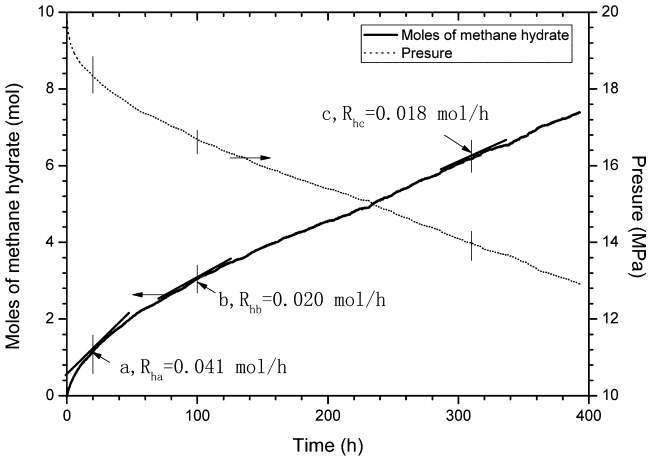

Figure 3. System pressure and the cumulative amount of hydrate formation for the reference case.

decreases when the experiment of hydrate formation begins. After 393.5 h of hydrate formation, 7.41 mol of methane hydrate are formed in the CHS and the system pressure decreases to 12.90 MPa. It is easy to calculate that the average rate of hydrate formation (R_{havg}) is 0.019 mol/h. However, the rate of formation during the formation process is varying. The formation rate is relatively high at the beginning of the experiment. Afterward, the rate gradually declines to a stable value. For example, the hydrate formation rate at point a (20th min) is 0.041 mol/h, which is higher than that at point b (100th min) of 0.020 mol/h. However, the formation rate decreases slightly from 0.020 mol/h (the point b, 100th min) to 0.018 mol/h (point c, 310th min). The hydrate formation is a complex process that occurs during heat and mass transfer with formation kinetics of hydrate. According to the kinetics equation of the hydrate formation,[29] the rate of hydrate formation is related to the fugacity difference (the difference between the fugacity of methane under local conditions and the fugacity at equilibrium). The bigger the fugacity difference leads to the higher rate of hydrate formation. The fugacity is usually replaced by local gas pressure. During the formation experiment, the temperatures in the CHS are 8.5 °C, approximately. The corresponding equilibrium pressure is calculated as 6.0 MPa, using the model by Li et al.[30] The system pressures for points a, b, and c are 18.33, 16.68, and 13.98 MPa, respectively. Thus, the fugacity differences for points a, b, and c are 12.33, 10.68, and 7.98 MPa, respectively. Obviously, the rates of hydrate formation are not in proportion to the fugacity differences, indicating that the fugacity difference is not the most important factor for the hydrate formation. A similar phenomenon has been reported by Kneafsey et al.[19]

Figure 4 shows the curves of temperatures in the CHS of the reference case. The thermocouples selected in Figure 4 are 1A, 1B, 1C, 13A, 13B, 13C, 25A, 25B, and 25C, which are on the diagonal face of the CHS. As seen in Figure 4, the temperatures instantly increase from initial temperature to about 11.0 °C and then decrease to 8.5 °C in the first 10 min. This is probably because the methane hydrate formation is an exothermic reaction and the rate of hydrate formation is relatively high at the beginning of the experiment. The heat of formation releases to the hydrate reservoir, causing the increase of the temperatures. Afterward, the heat diffuses to the water bath through the boundaries of the vessel and the rate of hydrate formation decreases, leading to the decline of temperatures. Furthermore,

dx.doi.org/10.1021/ef400720h | Energy Fuels 2013, 27, 3751−3757

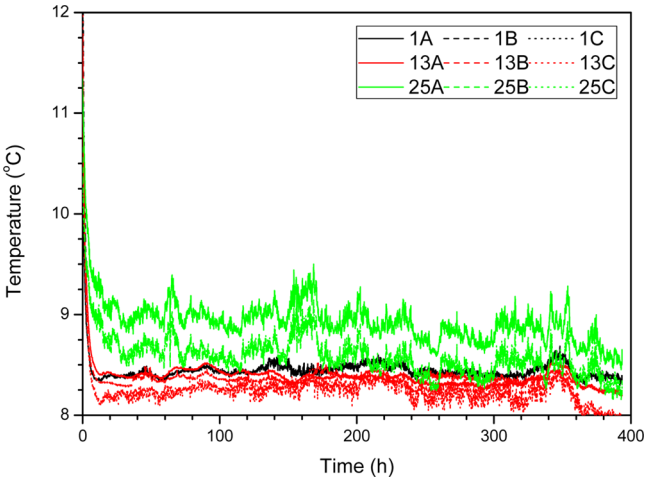

Figure 4. Curves of temperatures in the CHS of the reference case.

the changes of temperatures on the same vertical line are similar, such as the temperatures of 1A, 1B, and 1C. However, the temperatures on a diagonal line are different, such as the temperatures of 1A, 13A, and 25A. Moreover, the temperatures of 1A and 25A are higher than that of 13A. This indicates that the formation reaction in the boundary region is more intense than that in the center region, because the higher temperatures are caused by the heat released from the formation reaction. A similar phenomenon has been reported by Yang et al.[22]

The change of the gas hydrate reservoir can be characterized by the resistance, because the resistance increases with the hydrate formation.[31,32] In this work, the spatial distributions of the resistance ratio (the real-time resistance divided by the 0 min resistance during the experiment) are used for representing the hydrate formation behaviors in the CHS. Figure 5 shows the spatial distributions of the resistance ratio during the hydrate formation for the reference experiment. As seen in Figure 5, the resistance ratios gradually increase from the boundary regions to the center region, indicating that the hydrate forms from the boundaries to the center. This is consistent with the conclusion obtained from Figure 4.

3.2. Hydrate Formations in Different Volumes of Vessels. The vessels with different volumes (PHS, 5.8 L; CHS, 117.8 L) are used for investigating the effect of the volume on the hydrate formation. The porosities in the PHS and CHS are both 48%. Thus, the pore volume in the PHS is 20.3 times larger than that in the CHS. Before the experiments start, the initial volumes of gas/water in the PHS and CHS are 34222/21 144 mL and 1703/1049 mL, respectively. Therefore, the initial gas–water ratios (volume) for the experiments in the PHS and CHS are both 1.62 approximately. Figure 6 gives the cumulative amounts of hydrate formation in the CHS and PHS. As seen in Figure 6, methane hydrates of about 118.1 mol form in the PHS and about 5.2 mol of hydrate form in the CHS, in the same experimental times (250 h). The mole ratio of hydrate formation for the experiment of PHS and that of the CHS is calculated as 22.7, which is close to the ratio of the pore volume in the PHS and that in the CHS (20.3). As also indicated in Figure 6, at the 115th min, the rate of hydrate formation in the PHS is 0.40 mol/h, which is 20 times higher than that in the CHS (0.020 mol/h). Furthermore, the curves for the PHS and CHS are kept in parallel during most of the formation time (after 30 min), which indicates that the formation rate for the PHS is kept 20 times higher than that for the CHS during this period. Thus, the formation rate is directly proportional to the pore volume, indicating that the volume of porous media is one of the important factors on the hydrate formation.

3.3. Hydrate Formation with Different Initial Gas–Water Ratios. A total of five experiments of hydrate formation

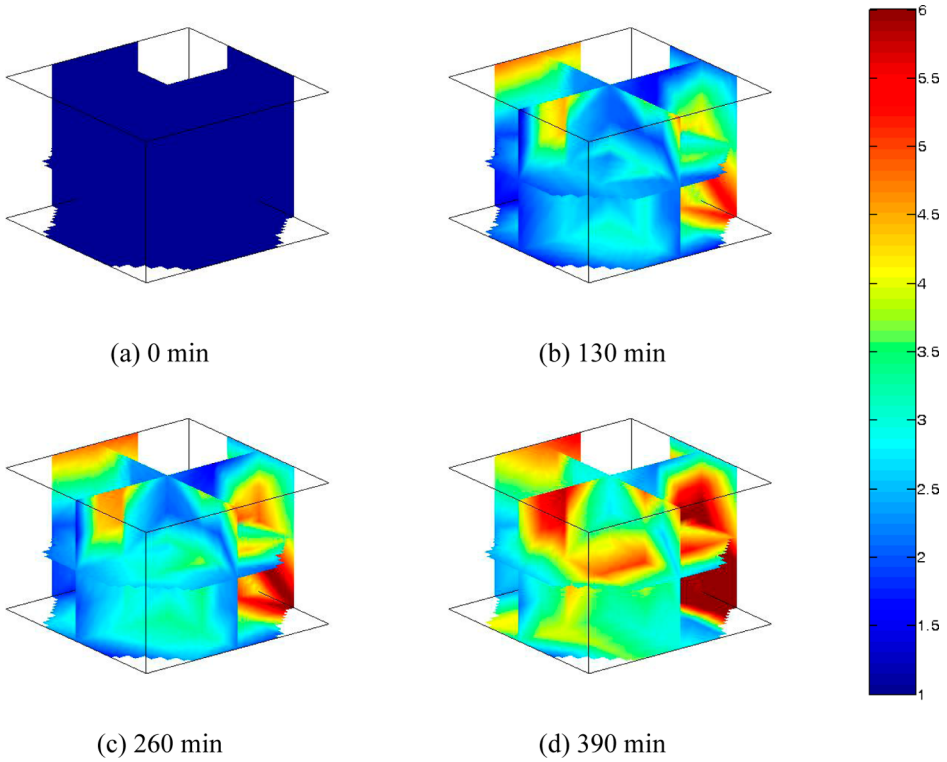

Figure 5. Spatial distributions of the resistance ratio during the hydrate formation for the reference experiment.

dx.doi.org/10.1021/ef400720h | *Energy Fuels* 2013, 27, 3751–3757

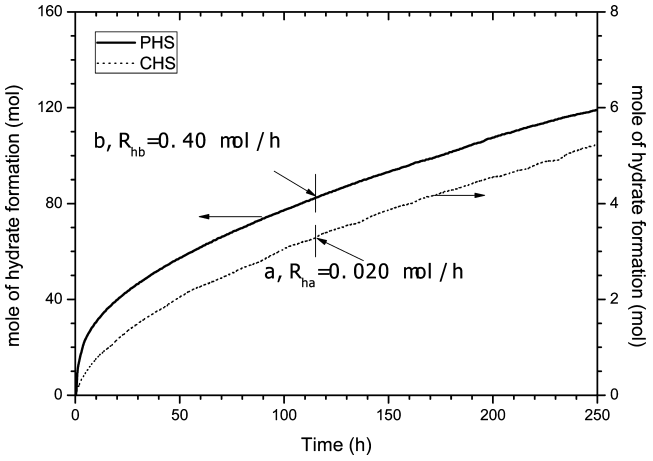

Figure 6. Cumulative amounts of hydrate formation in the CHS and PHS.

with different initial gas–water ratios are carried out in this work. During these experiments, the initial pressures before the hydrate formation and the final pressures after the hydrate formation are all 20.0 and 13.5 MPa, respectively. The conditions and results of these experiments are listed in Table 1, including the initial amounts of water and methane,

Table 1. Conditions and Results of the Methane Hydrate Formation with Different Initial Gas–Water Ratios

initial gas–water ratio	initial amount of water (mL)	initial amount of methane (mol)	cumulative amount of hydrate formation (mol)	time (h)	conversions of gas to hydrate (%)
0.79	1539	12.61	4.11	134	32.6
1.10	1311	15.63	5.66	238	36.2
1.31	1192	17.21	6.46	313	37.5
1.62	1049	18.49	6.75	349	36.5
2.93	701	22.03	7.87	371	35.7

the cumulative amount of hydrate formation, the time for hydrate formation, and the conversions of gas to hydrate. As shown in Table 1, the initial gas–water ratios (volume) for these experiments are 0.79, 1.10, 1.31, 1.62, and 2.93, respectively. Although the pressure drops for these experiments are the same (6.5 MPa), the time consumed for the hydrate formations are different, which are proportional to the initial gas–water ratios. Furthermore, the final mole of hydrate formation increases with the increase of the time. However, the conversions of gas to hydrate are similar in these experiments, because the pressure drops for these experiments are all the same. Figure 7 shows the curves of the cumulative amount of hydrate formation with different gas–water ratios in the CHS. As seen in Figure 7, the curves overlap, which indicates that the rates of hydrate formation for these experiments are similar. Thus, the change of the initial gas–water ratio has little effect on the rate of hydrate formation. However, with the same pressure drop, the higher initial gas–water ratio leads to the larger amount of hydrate formation, causing the longer formation time.

3.4. Hydrate Formation with High Hydrate/Water Saturation and Low Gas Saturation. In this work, a hydrate sample with the hydrate saturation of 42%, the water saturation of 44%, and gas saturation of 14% is prepared to obtain in the

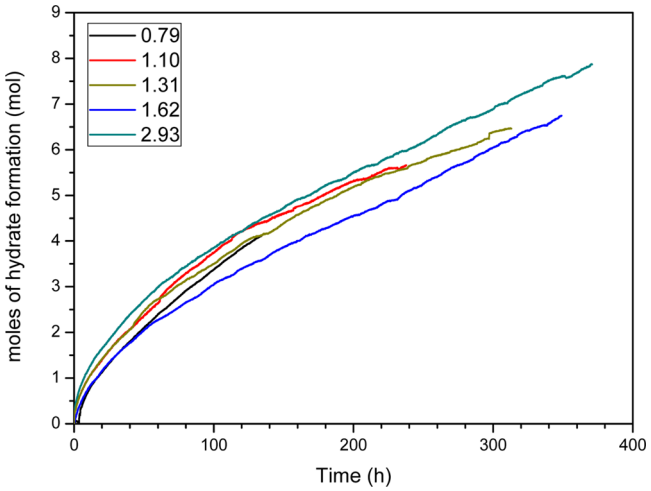

Figure 7. Cumulative amounts of hydrate formation with different gas–water ratios in the CHS.

vessel of PHS. According to the method, which has been described in section 2.2.2, the initial amounts of the methane (N_g^0) and water (N_w^0) are calculated to be 224.9 and 2236.6 mol, respectively. The water volume of 2207.9 mol is 40 259.0 mL. If all gas and water are compressed into the PHS, the system pressure will increase to about 39.5 MPa, which is much higher than the extreme design pressure. Thus, the water and gas should be injected by multiphases. First, all methane (224.9 mol) and a part of water (29 594.1 mL) are injected into the vessel to pressurize the system to 20 MPa. Afterward, when the pressure declines to about 15 MPa, a certain volume of water is injected into the vessel to pressurize the system to 20 MPa. During this experiment, the rest of water (10 664.9 mL) is injected into the system with three injections. The volumes of water for each injection are 4901.6, 3435.5, and 2327.8 mL, sequentially. Finally, the hydrate sample with the designed three-phase saturations is obtained by these experimental processes. Thus, when the predetermined saturations are changed, the hydrate samples with any designed gas/water/hydrate saturation can be synthesized. The curves of gas/water/hydrate saturations and system pressure for the experiment are shown in Figure 8. As seen in Figure 8, there are three abrupt

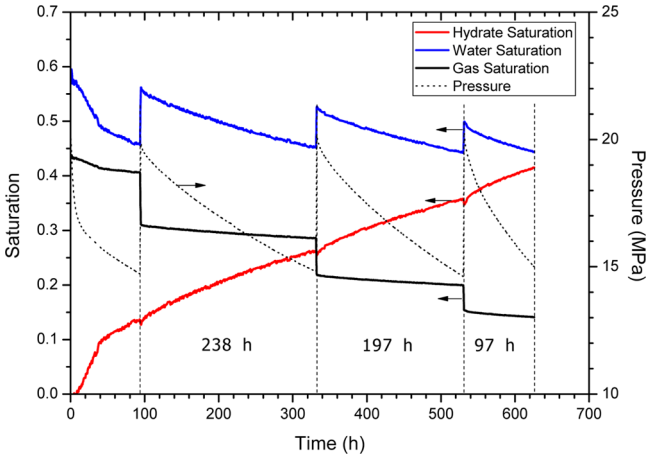

Figure 8. Curves of gas/water/hydrate saturations and system pressure for the experiment of hydrate formation with high hydrate/water saturation and low gas saturation.

dx.doi.org/10.1021/ef400720h | *Energy Fuels* 2013, 27, 3751–3757

changes for the curves, which are caused by the water injections. At each injection, the water saturation and pressure increase dramatically and the gas saturation decreases suddenly. However, the hydrate saturation changes little, because little hydrate is dissociated during the injection. During the whole process of the experiment, the rate of hydrate formation is kept at a relatively stable value, because the effect of the gas−water ratio and the system pressure on the formation rate is limited, which has been discussed in Figures 3 and 7. Meanwhile, as the gas−water ratio decreases, the formation time with a constant pressure drop decreases. This phenomenon is in accordance with that in Figure 7.

Therefore, the advantages of the new method for the hydrate formation with high hydrate/water saturation and low gas saturation are (1) the hydrate sample with any designed gas/water/hydrate saturation can be obtained; (2) the rate of hydrate formation is stable during the experiment; and (3) the extreme design pressure of the vessel can be reduced, further reducing the manufacturing cost.

4. CONCLUSION

In this work, the methane hydrate formation in porous media was investigated in three-dimensional (3D) vessels. Meanwhile, a new method was designed to form methane hydrate samples in porous sediments with high hydrate/water saturation and low gas saturation. The following conclusions are obtained:

The rates of hydrate formation are not always proportional to the fugacity differences. However, the volume of porous media is one of the important factors, and the formation rate increases with the pore volume. Moreover, the change of the initial gas−water ratio has little effect on the rate of hydrate formation, while the higher initial gas−water ratio leads to the larger amount of hydrate formation and the longer formation time with the same pressure drop.

According to the discussion about the temperatures and resistances in hydrate reservoir, it is confirmed that the hydrate forms from the boundaries to the center.

The original method for the hydrate formation with high hydrate/water saturation and low gas saturation is successful in this work. Using this method, the hydrate sample with any designed gas/water/hydrate saturation can be obtained.

■ AUTHOR INFORMATION

Corresponding Author

*Telephone: +86-20-87057037. Fax: +86-20-87034664. E-mail: lixs@ms.giec.ac.cn.

Notes

The authors declare no competing financial interest.

■ ACKNOWLEDGMENTS

This work is supported by the National Science Fund for Distinguished Young Scholars of China (51225603), the National Natural Science Foundation of China (51076155 and 51106160), and Science & Technology Program of Guangzhou City (2012J5100012), which are gratefully acknowledged.

■ REFERENCES

(1) Sloan, E. D. *Clathrate Hydrates of Natural Gases*; Marcel Dekker, Inc.: New York, 1998.

(2) Sloan, E. D. Fundamental principles and applications of natural gas hydrates. *Nature* **2003**, *426* (6964), 353−359.

(3) Li, X. S.; Yang, B.; Li, G.; Li, B. Numerical simulation of gas production from natural gas hydrate using a single horizontal well by depressurization in Qilian Mountain permafrost. *Ind. Eng. Chem. Res.* **2012**, *51* (11), 4424−4432.

(4) Li, G.; Moridis, G. J.; Zhang, K.; Li, X. S. The use of huff and puff method in a single horizontal well in gas production from marine gas hydrate deposits in the Shenhu Area of South China Sea. *J. Pet. Sci. Eng.* **2011**, *77* (1), 49−68.

(5) Chand, S.; Minshull, T. A. The effect of hydrate content on seismic attenuation: A case study for Mallik 2L-38 well data, Mackenzie delta, Canada. *Geophys. Res. Lett.* **2004**, *31* (14), 1−4.

(6) Koh, C. A.; Sloan, E. D.; Sum, A. K.; Wu, D. T. Fundamentals and applications of gas hydrates. *Annu. Rev. Chem. Biomol. Eng.* **2011**, *2* (2), 237−257.

(7) Castaldi, M. J.; Zhou, Y.; Yegulalp, T. M. Down-hole combustion method for gas production from methane hydrates. *J. Pet. Sci. Eng.* **2007**, *56* (1−3), 176−185.

(8) Li, X. S.; Wan, L. H.; Li, G.; Li, Q. P.; Chen, Z. Y.; Yan, K. F. Experimental investigation into the production behavior of methane hydrate in porous sediment with hot brine stimulation. *Ind. Eng. Chem. Res.* **2008**, *47* (23), 9696−9702.

(9) Makogon, T. Y.; Larsen, R.; Knight, C. A.; Sloan, E. D. Melt growth of tetrahydrofuran clathrate hydrate and its inhibition: Method and first results. *J. Cryst. Growth* **1997**, *179* (1−2), 258−262.

(10) Li, X. S.; Zhang, Y.; Li, G.; Chen, Z. Y.; Wu, H. J. Experimental investigation into the production behavior of methane hydrate in porous sediment by depressurization with a novel three-dimensional cubic hydrate simulator. *Energy Fuels* **2011**, *25* (10), 4497−4505.

(11) Ahmadi, G.; Ji, C. A.; Smith, D. H. Production of natural gas from methane hydrate by a constant downhole pressure well. *Energy Convers. Manage.* **2007**, *48* (7), 2053−2068.

(12) Li, X. S.; Yang, B.; Zhang, Y.; Li, G.; Duan, L. P.; Wang, Y.; Chen, Z. Y.; Huang, N. S.; Wu, H. J. Experimental investigation into gas production from methane hydrate in sediment by depressurization in a novel pilot-scale hydrate simulator. *Appl. Energy* **2012**, *93*, 722−732.

(13) Li, G.; Li, X. S.; Tang, L. G.; Zhang, Y. Experimental investigation of production behavior of methane hydrate under ethylene glycol injection in unconsolidated sediment. *Energy Fuels* **2007**, *21* (6), 3388−3393.

(14) Hirohama, S.; Shimoyama, Y.; Wakabayashi, A.; Tatsuta, S.; Nishida, N. Conversion of CH_4-hydrate to CO_2-hydrate in liquid CO_2. *J. Chem. Eng. Jpn.* **1996**, *29* (6), 1014−1020.

(15) Hensen, C.; Wallmann, K. Methane formation at Costa Rica continental margin—Constraints for gas hydrate inventories and cross-decollement fluid flow. *Earth Planet. Sci. Lett.* **2005**, *236* (1−2), 41−60.

(16) Hickman, S. H.; Hsieh, P. A.; Mooney, W. D.; Enomoto, C. B.; Nelson, P. H.; Mayer, L. A.; Weber, T. C.; Moran, K.; Flemings, P. B.; McNutt, M. K. Scientific basis for safely shutting in the Macondo Well after the April 20, 2010 Deepwater Horizon blowout. *Proc. Natl. Acad. Sci. U.S.A.* **2012**, *109* (50), 20268−20273.

(17) Christiansen, R. L.; Sloan, E. D. Mechanisms and kinetics of hydrate formation. *Int. Conf. Nat. Gas Hydrates* **1994**, *715*, 283−305.

(18) Kvamme, B. Kinetics of hydrate formation from nucleation theory. *Int. J. Offshore Polar Eng.* **2002**, *12* (4), 256−263.

(19) Kneafsey, T. J.; Tomutsa, L.; Moridis, G. J.; Seol, Y.; Freifeld, B. M.; Taylor, C. E.; Gupta, A. Methane hydrate formation and dissociation in a partially saturated core-scale sand sample. *J. Pet. Sci. Eng.* **2007**, *56* (1−3), 108−126.

(20) Linga, P.; Haligva, C.; Nam, S. C.; Ripmeester, J. A.; Englezos, P. Gas hydrate formation in a variable volume bed of silica sand particles. *Energy Fuels* **2009**, *23*, 5496−5507.

(21) Zhou, Y.; Castaldi, M. J.; Yegulalp, T. M. Experimental investigation of methane gas production from methane hydrate. *Ind. Eng. Chem. Res.* **2009**, *48* (6), 3142−3149.

(22) Yang, X.; Sun, C. Y.; Su, K. H.; Yuan, Q.; Li, Q. P.; Chen, G. J. A three-dimensional study on the formation and dissociation of methane

hydrate in porous sediment by depressurization. *Energy Convers. Manage.* **2012**, *56*, 1−7.
(23) Boswell, R.; Collett, T. S. Current perspectives on gas hydrate resources. *Energy Environ. Sci.* **2011**, *4* (4), 1206−1215.
(24) Li, X. S.; Wang, Y.; Li, G.; Zhang, Y.; Chen, Z. Y. Experimental investigation into methane hydrate decomposition during three-dimensional thermal huff and puff. *Energy Fuels* **2011**, *25* (4), 1650−1658.
(25) Li, X. S.; Yang, B.; Li, G.; Li, B.; Zhang, Y.; Chen, Z. Y. Experimental study on gas production from methane hydrate in porous media by huff and puff method in pilot-scale hydrate simulator. *Fuel* **2012**, *94*, 486−494.
(26) Li, X. S.; Wang, Y.; Duan, L. P.; Li, G.; Zhang, Y.; Huang, N. S.; Chen, D. F. Experimental investigation into methane hydrate production during three-dimensional thermal huff and puff. *Appl. Energy* **2012**, *94*, 48−57.
(27) Li, X. S.; Wang, Y.; Li, G.; Zhang, Y. Experimental investigations into gas production behaviors from methane hydrate with different methods in a cubic hydrate simulator. *Energy Fuels* **2011**, *26* (2), 1124−1134.
(28) Li, G.; Li, X. S.; Wang, Y.; Zhang, Y. Production behavior of methane hydrate in porous media using huff and puff method in a novel three-dimensional simulator. *Energy* **2011**, *36* (5), 3170−3178.
(29) Sun, X. F.; Mohanty, K. K. Kinetic simulation of methane hydrate formation and dissociation in porous media. *Chem. Eng. Sci.* **2006**, *61* (11), 3476−3495.
(30) Li, X. S.; Zhang, Y.; Li, G.; Chen, Z. Y.; Yan, K. F.; Li, Q. P. Gas hydrate equilibrium dissociation conditions in porous media using two thermodynamic approaches. *J. Chem. Thermodyn.* **2008**, *40* (9), 1464−1474.
(31) Ren, S. R.; Liu, Y. J.; Liu, Y. X.; Zhang, W. D. Acoustic velocity and electrical resistance of hydrate bearing sediments. *J. Pet. Sci. Eng.* **2010**, *70* (1−2), 52−56.
(32) Zhou, X. T.; Fan, S. S.; Liang, D. Q.; Wang, D. L.; Huang, N. S. Use of electrical resistance to detect the formation and decomposition of methane hydrate. *J. Nat. Gas Chem.* **2007**, *16* (4), 399−403.